



HAL
open science

Fluid coating from a polymer solution

Alain de Ryck, D Quere

► **To cite this version:**

Alain de Ryck, D Quere. Fluid coating from a polymer solution. *Langmuir*, 1998, 14 (7), pp.1911-1914.
10.1021/la970584r . hal-01652394

HAL Id: hal-01652394

<https://hal.science/hal-01652394>

Submitted on 8 Nov 2019

HAL is a multi-disciplinary open access archive for the deposit and dissemination of scientific research documents, whether they are published or not. The documents may come from teaching and research institutions in France or abroad, or from public or private research centers.

L'archive ouverte pluridisciplinaire **HAL**, est destinée au dépôt et à la diffusion de documents scientifiques de niveau recherche, publiés ou non, émanant des établissements d'enseignement et de recherche français ou étrangers, des laboratoires publics ou privés.

Fluid Coating from a Polymer Solution

Alain de Ryck[†] and David Quéré^{*,‡}

École des Mines d'Albi, route de Teillet, 81013 Albi CT Cedex 09, France, and Laboratoire de Physique de la Matière Condensée, URA 792 du CNRS, Collège de France, 75231 Paris Cedex 05, France

New experiments on coating of a wire with aqueous poly(ethylene oxide) solutions are reported. If these experiments are compared with coating with a pure liquid of the same physical characteristics, a strong thickening of the liquid layer is observed. This effect is described by considering the normal stresses, which allows us to obtain an analytical expression for the coated thickness in good agreement with the data.

1. Introduction

Fluid coating is a process of practical importance in numerous industrial contexts, which consists of drawing a solid out of a bath of liquid (or conversely in moving a liquid on a fixed solid). First studied by Goucher and Ward,¹ this problem was modeled by Landau, Levich, and Derjaguin.^{2,3} If the solid is a thin fiber (of radius b much smaller than the capillary length $\kappa^{-1} = (\gamma/\rho g)^{1/2}$, where γ and ρ are the surface tension and specific mass of the liquid and g is the acceleration of gravity), the thickness e of the coated layer is given by

$$e = 1.34bCa^{2/3} \quad (1)$$

where Ca is the capillary number, which compares the viscous forces to the capillary ones: $Ca = \eta V/\gamma$, with η being the viscosity of the liquid and V the withdrawal velocity of the fiber from the liquid bath.

We have recently checked the validity of eq 1 at small capillary numbers.⁴ In addition, we have shown that for high withdrawal velocities (above typically 1 m/s), the film thickness increases faster with Ca than predicted by eq 1, because of the liquid inertia which tends to eject the liquid out of the reservoir. Here, we present an experimental study of the coating at low velocity (where eq 1 is supposed to be valid) by a polymer solution. Then, a model is proposed in order to understand the data.

2. Experiments

The experiments were achieved with nickel wires of radius $b = 63.5 \mu\text{m}$ and aqueous solutions of poly(ethylene oxide) (PEO) of molecular weight of $M = 4 \times 10^6$ g. The corresponding overlap concentration c^* is 10^{-4} g/g. Five concentrations were used: 10^{-5} , 10^{-4} , 10^{-3} , 5×10^{-3} , 10^{-2} (all expressed in g/g), thus lying below, around, and above c^* . The polymer, purchased from Aldrich, was used without further purification and dissolved in tridistilled water by softly shaking (24 h) and then warming (1 h) at 50°C to prevent the formation of aggregates.⁵ The surface tensions were measured by the ring method and the viscosities estimated by an Ostwald viscometer. All these characteristics are summarized in Table 1.

Table 1. Characteristics of the PEO Solutions Used in This Study^a

% concn (g/g)	γ (mN/m)	viscosimeter		experiment	
		η (mPa·s)	$\dot{\gamma}$ (s ⁻¹)	V/e (s ⁻¹)	η (mPa·s)
0.001	60.5	1.1	500	17000–170000	1.1
0.01	61.6	1.2	500	9700–32000	1.2
0.1	61.7	2.7	180	1940–6200	1.7–1.9
0.5	61.7	37.3	10	1720–1800	8–9
1	61.8	515	1	680–870	38–225

^a The concentration is given in mass (the overlap concentration being $c^* = 0.01\%$). For each solution, surface tension and viscosity are measured and reported; the shear rate corresponding to the viscosity measurement is indicated, and the one endured by the liquid during the experiments is evaluated (it is of order V/e , where both the withdrawal viscosity V and the film thickness e are measured), from which the actual viscosity can be evaluated thanks to ref 6.

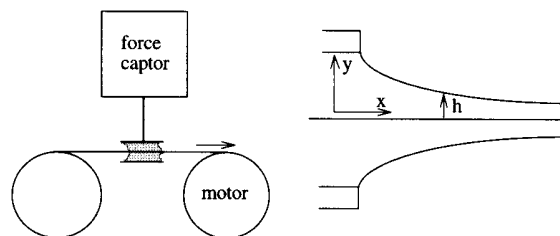


Figure 1. Experimental setup for measuring the thickness of the film entrained by a fiber drawn out of a reservoir and sketch of the region where the film forms (so-called dynamic meniscus).

Actually, the solutions above c^* are non-Newtonian and their viscosities depend on the shear rate $\dot{\gamma}$: at high $\dot{\gamma}$, the viscosity decreases with $\dot{\gamma}$ because the flow disentangles the polymer. Powell and Schwarz⁶ provided extensive data for the $\eta(\dot{\gamma})$ dependence for various concentrations of water solutions of PEO of comparable molecular weight. Thanks to these data, we could estimate the actual viscosity for each experiment, taking a shear rate (at the place where the film forms) of order V/e , where both V and e were measured. The intervals for the shear rate and the viscosity are also reported in Table 1.

The wires were coated by pulling them through a reservoir (a Teflon tube of length 1.5 cm and radius 2 mm) at a constant speed V , as pictured in Figure 1. The thickness of the coated layer was measured by continuously weighting the reservoir. Results are displayed in Figure 2. The film thickness (normalized by the wire radius) is plotted as a function of the capillary number,

(6) Powell, R. L.; Schwartz, W. H. *Rheol. Acta* **1975**, *14* 729.

[†] École des Mines d'Albi.

[‡] Collège de France.

(1) Goucher, F. S.; Ward, H. *Philos. Mag.* **1922**, *44*, 1002.

(2) Landau, L.; Levich, B. *Acta Physicochim. USSR* **1942**, *17*, 42.

(3) Derjaguin, B. *Acta Physicochim. USSR* **1943**, *20*, 349.

(4) De Ryck, A.; Quéré, D. *J. Fluid Mech.* **1996**, *311*, 219.

(5) Cabane, B.; Duplessix, R. *J. Phys. (Paris)* **1987**, *48*, 651.

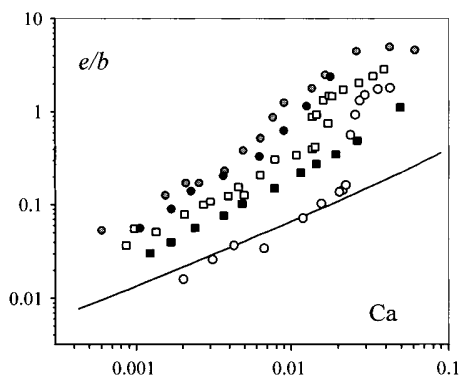


Figure 2. Dimensionless thickness e/b vs the capillary number for five different concentrations (empty circles, $c = 0.001\%$; empty squares, $c = 0.01\%$; gray circles, $c = 0.1\%$; full circles, $c = 0.5\%$; full squares, $c = 1\%$; overlap concentration c^* is 0.01%). The capillary number is calculated by evaluating the shear rate in the dynamic meniscus and then considering the dynamic viscosity at this rate. The full line is the Landau law (eq 1).

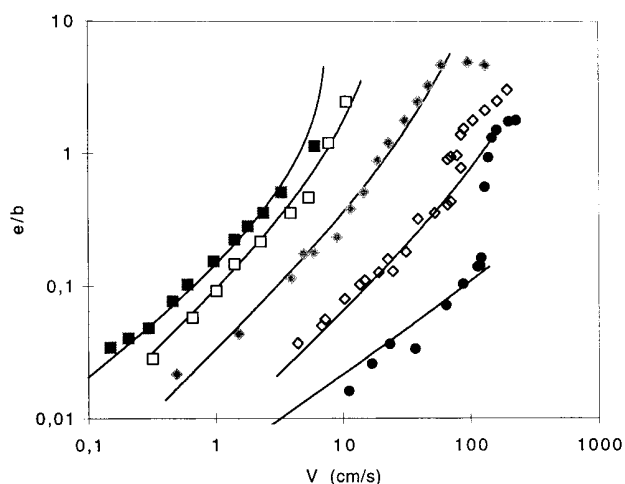


Figure 3. Dimensionless thickness e/b vs the withdrawal velocity. The data are the ones of Figure 2 (empty rhombi, $c = 0.01\%$; full rhombi, $c = 0.1\%$; empty squares, $c = 0.5\%$; full squares, $c = 1\%$). The full lines are the fits provided by eq 22. For the dilute solution (full circles, $c = 0.001\%$), the line is the Landau law (eq 1 or eq 22 with $n = 1$ and $N = 0$).

calculated with the viscosity estimated as explained above. In the same figure, the Landau law (eq 1) is drawn and compared with the data.

In all cases, the thickness is found to increase with the velocity. For the dilute solution ($c = 10^{-5}$ g/g), the data (empty circles) are close to the Landau law at small capillary number. Then, above a threshold ($Ca \approx 0.025$ or $V \approx 1.3$ m/s), the film thickness sharply increases with the velocity, which is a consequence of inertia;⁴ the same inertial behavior can be observed around $V = 1$ m/s with the solution $c = 10^{-4}$ g/g. This divergence does not occur with the other solutions, which are of higher viscosity, so that the withdrawal velocities are smaller. Note finally that when the thickness becomes larger than the wire radius, some saturation occurs, because of the finite size of the reservoir (see ref 4 for a detailed analysis).

The new effect observed in Figure 2 is that, even at small capillary numbers, data corresponding to semidilute solutions ($c \geq c^*$) are systematically above the Landau law: *the presence of the polymer causes a swelling of the film*. The swelling factor (ratio of the actual thickness over the Landau one) varies between 2 and 8. In addition, it depends on the capillary number: the thickness is roughly proportional to the velocity (in particular at small V , where the thickness is much smaller than the wire radius), which can be seen in Figure 3 where the same data are displayed directly vs the withdrawal velocity.

3. A Model

3.1. General Equations. We interpret the swelling of the film as a consequence of the *Weissenberg effect*, which appears when the characteristic time for the flow (e/V) is smaller than the characteristic time of response of the material (the reptation time, for a semidilute solution). A spectacular manifestation of the Weissenberg effect (also called *normal stress effect*) is that jets of polymer solutions expand rather than shrink when going out of a tube (see ref 7 for example). Because of the normal stress, we qualitatively understand that the coated layer is thicker than expected, as seen in Figure 2. We propose to quantify it by incorporating this effect in the equations of movement, as in ref 8 where normal stresses were introduced for predicting the thickness of a soap film drawn out of a solution containing polymer. For small thicknesses, we can work in Cartesian coordinates.

Using the notations of Figure 1, the stress tensor is written as

$$\sigma = \begin{pmatrix} \tau_{xx} & \tau_{xy} & 0 \\ \tau_{yx} & \tau_{yy} & 0 \\ 0 & 0 & \tau_{zz} \end{pmatrix} \quad (2)$$

with $\tau_{xy} = \eta(\partial u/\partial y)$. For a Newtonian liquid, η is independent of the shear rate, but for a polymeric solution, it can be empirically written

$$\eta = \begin{cases} \eta_0 & \text{if } \dot{u} < \dot{u}_c \\ k \left| \frac{\partial u}{\partial y} \right|^{n-1} & \text{if } \dot{u} > \dot{u}_c \end{cases} \quad (3)$$

where η_0 , k , and n are constants which may be determined experimentally. The diagonal terms contain the pressure ($\tau_{xx} + \tau_{yy} + \tau_{zz} = -3p$). For a Newtonian liquid, we have: $\tau_{xx} = \tau_{yy} = \tau_{zz} = -p$. With normal stresses, we only have

$$\tau_{yy} - \tau_{zz} = 0 \quad (4)$$

and we can define

$$\zeta = \frac{\tau_{xx} - \tau_{yy}}{\left(\frac{\partial u}{\partial y}\right)^2} \quad (5)$$

In addition and very generally, ζ is proportional to η^2 .⁹ So, the tensor matrix can finally be written

$$\sigma = \begin{pmatrix} -p + N\left(\frac{\partial u}{\partial y}\right)^{2n} & \eta \frac{\partial u}{\partial y} & 0 \\ \eta \frac{\partial u}{\partial y} & -p - \frac{1}{2}N\left(\frac{\partial u}{\partial y}\right)^{2n} & 0 \\ 0 & 0 & -p - \frac{1}{2}N\left(\frac{\partial u}{\partial y}\right)^{2n} \end{pmatrix} \quad (6)$$

defining the *normal stress coefficient* N . Then, the steady Navier–Stokes equation is written in the lubrication approximation

(7) Bird, R. B.; Armstrong, R. C.; Hassager, O. *Dynamics of polymeric liquids*; John Wiley: New York, 1977.

(8) Bruinsma, R.; di Meglio, J. M.; Quéré, D.; Cohen-Addad, S. *Langmuir* **1992**, *8*, 3161.

(9) Ferry, J. D. *Viscoelastic Properties of Polymers*; John Wiley: New York, 1980.

$$\frac{\partial p}{\partial x} = \frac{\partial}{\partial y} \left[k \left| \frac{\partial u}{\partial y} \right|^{n-1} \frac{\partial u}{\partial y} \right] + \frac{\partial}{\partial x} \left[N \left(\frac{\partial u}{\partial y} \right)^{2n} \right] \quad (7)$$

where we have supposed that the shear rate is larger than its critical value (see eq 3). The pressure inside the film is given by the Laplace law, which writes for smooth profiles: $p = -\gamma d^2h/dx^2$. If the liquid were pure, the flow at small velocities would be a Poiseuille flow, with a parabolic profile inside the film. We suppose that introducing the polymer keeps the flow close to a Poiseuille one, and write

$$u(x,y) = V + A(x) \left(\frac{y^2}{2} - yh \right) \quad (8)$$

where h is the thickness of the liquid layer at the place where the film forms (see Figure 1). A is determined by the flux conservation: $A = 3V(h - e)/h^3$. After the dimensionless variables are introduced, $x = lX$ (l is the characteristic length of formation of the film) and $h = eY$, the y -variable is eliminated by an average on the thickness in eq 7 (a method first proposed in ref 10). Thus, we obtain

$$Y''' = - \left\{ \frac{k(3V)^n l^3}{e^{n+2} \gamma} \right\} \frac{(Y-1)^n}{Y^{2n+1}} + \left\{ \frac{2n}{2n+1} \frac{N(3V)^{2n} l^2}{\gamma e^{2n+1}} \right\} \frac{(Y-1)^{2n-1} (3-2Y)}{Y^{4n+1}} Y' \quad (9)$$

where the sign ' represents a derivation with respect to X . By choosing l in order to make the first coefficient equal to 1 and calling B the second one, we can reduce eq 9 to

$$Y''' = - \frac{(Y-1)^n}{Y^{2n+1}} + B \frac{(Y-1)^{2n-1} (3-2Y)}{Y^{4n+1}} Y' \quad (10)$$

The thickness e is then obtained by using the matching condition proposed by Landau.^{2,11} We write that the curvature of the film tends to zero in the direction of the reservoir:

$$\frac{1}{b+e} = \frac{e}{l^2} Y'' \Big|_{Y \rightarrow \infty} \quad (11)$$

Thus, the end of the calculation consists of integrating once eq 10 and looking for the limit written in eq 11. Before proposing an approximate solution, we first derive simple scaling arguments.

3.2. Scaling Laws. The searched limit in eq 11 is a number, so that the matching condition dimensionally is written as

$$l \approx \sqrt{e(b+e)} \quad (12)$$

Then, we propose to treat separately the two non-Newtonian terms of the right member of eq 7. First, if we have $N = 0$ (no normal stress), eq 7 dimensionally reads

$$\gamma \frac{e}{l^3} \approx k \frac{V^n}{e^{n+1}} \quad (13)$$

where the characteristic lengths along x and y (respectively l and e) were introduced. From eqs 12 and 13, we deduce the scaling law for the thickness as a function of the velocity

$$e \approx \left(\frac{b^3 k^2}{\gamma^2} \right)^{1/(2n+1)} V^{2n/(2n+1)} \quad (14)$$

where we have supposed that the thickness is smaller than the fiber radius. Equation 14 should be valid for shear rates larger than \dot{u}_c (see eq 3), which implies capillary numbers larger than $Ca^* = (\dot{u}_c \eta_0 b / \gamma)^3$. For capillary numbers smaller than Ca^* , the Landau equation should be obeyed. Thus, as Ca increases, the film thickness should successively follow eqs 1 and 14. Since we have $n < 1$, the exponent in eq 14 is smaller than $2/3$, which means that the effect of shear thinning is (logically) to make the film thinner than predicted by Landau—a situation which was not observed in our experiments.

Conversely, if we only consider in eq 7 the term containing the normal stress, the latter equation dimensionally is written as

$$\gamma \frac{e}{l^3} \approx \frac{N}{l} \left(\frac{V}{e} \right)^{2n} \quad (15)$$

Eliminating l with eq 12 (and supposing $e \ll b$) leads to a linear variation for the thickness as a function of the velocity:

$$e \approx \left(\frac{Nb}{\gamma} \right)^{1/2n} V \quad (16)$$

The film thickness is found to be linear with the velocity, in accord with the observations at small velocity in Figure 3. As V increases, the experimental curves bend and exhibit some kind of slow divergence. It can simply be understood as a curvature effect: the thickness increases with the velocity and does not remain negligible, compared with the radius. Thus, b in eq 16 must be replaced by $(b+e)$ in eq 16, providing an implicit equation for the film thickness which implies a smooth divergence. For example, taking $n = 0.5$ (a case close to the most concentrated of our solutions; see Table 3) yields an hyperbolic divergence for the film thickness, which can be written as

$$e \approx \left(\frac{Nb}{\gamma} \right) \left(\frac{V}{1 - NV/\gamma} \right) \quad (17)$$

Thus, the scaling laws allow us to understand qualitatively the effect observed in the data. We can try now to derive more quantitative predictions by carrying on the calculation presented above.

3.3. Numerical Solution. The scaling analysis suggests that we should treat separately the non-Newtonian effect contained in eq 10 (shear thinning on one hand and normal stress on the other one). For the first term, the work was done by Gutfinger and Tallmadge,¹² who integrated numerically once eq 10 (without the second term: $B = 0$). They found for the limit

$$Y'' \Big|_{Y \rightarrow \infty} = 0.646 - 0.76 \ln n \quad (18)$$

where the first number is the Landau limit. From this point, the thickness dependence on the velocity could be derived, leading to the scaling behavior presented in eq 14.

Fully considered and integrated once, eq 10 can be written as

(10) White, D. A.; Tallmadge, J. A. *AICHE J.* **1966**, *12*, 333.
(11) Esmail, M. N.; Hummel, R. L. *AICHE J.* **1975**, *21*, 958.

(12) Gutfinger, C.; Tallmadge, J. A. *AICHE J.* **1965**, *11*, 403.

Table 2. Value of the Integral $I(n)^a$

n	$I(n)$
0.5	$1/2$
0.7	0.23
1	$1/12$

^a Which appears in eq 19 and is defined in eq 20, for the three different values of N , the exponent for the decreasing of the viscosity vs the shear rate (see eq 3), where $N = 1$ is the case of a Newtonian fluid.

Table 3. Values of the Non-Newtonian Parameters for the Different Solutions^a

% concn	k	n	$\dot{\gamma}_c$ (s ⁻¹)	N_{theo}	N_{exp}
0.001	0.01	1			0
0.01	0.012	1			2×10^{-5}
0.1	0.033	0.98	24	5×10^{-4}	9×10^{-4}
0.5	0.85	0.7	9	0.07	0.35
1	10	0.52	2	3.2	4.7

^a k , n , and $\dot{\gamma}_c$ (all defined in eq 3) are given in ref 6. Equation 23 allows us to calculate N_{theo} which is compared with the N_{exp} value provided by the fit in figure 3.

$$Y''|_{Y \rightarrow \infty} = \int_{-\infty}^{+\infty} \frac{(Y-1)^n}{Y^{2n+1}} dX + BI(n) \quad (19)$$

with

$$I(n) = \int_1^{+\infty} \frac{(2x-3)(x-1)^{2n-1}}{x^{4n+1}} dx \quad (20)$$

Table 2 gives some values for this integral. But the problem remains hard to solve, since the coefficient B depends on the (unknown) thickness e . We propose as an approximate solution to decouple the shear-thinning effect and the normal stress effect. Thus we simply modify eq 18 with the term calculated in eq 20, which can be written as

$$Y''|_{Y \rightarrow \infty} = 0.646 - 0.76 \ln n + BI(n) \quad (21)$$

Together with eq 11, the latter equation provides an expression for the thickness e :

$$\frac{1}{b+e} = (0.646 - 0.76 \ln n) \left\{ \frac{k(3V)^n}{e^{n+1/2}\gamma} \right\}^{2/3} + \frac{2n}{(2n+1)} I(n) \frac{N}{\gamma} \left(\frac{3V}{e} \right)^{2n} \quad (22)$$

This implicit equation can be drawn, since the values for k and n are known for our experimental solutions (these data come from ref 6 and are reported in Table 3). N only is treated as an adjustable parameter, and the best fits with the data provided by eq 22 are finally displayed in

Figure 3 (full lines). The agreement between the calculated curves and the experimental data appears to be good. In particular, the scaling features predicted in eqs 16 and 17 are well described by eq 22 (linearity at small capillary number and smooth divergence as the thickness becomes of order the fiber radius).

It remains to check that the values for the normal stress coefficient N deduced from the fit are reasonable. N can be evaluated independently: as emphasized above, the coefficient ζ defined in eq 5 is proportional to η^2 . Dimensionally, a pressure is missing. We can write $\zeta \approx \eta^2/\tau^*$, where τ^* is the threshold in stress above which the disentanglement occurs. Since we have $\tau^* \approx \eta_0 \dot{\gamma}_c \approx k \dot{\gamma}_c^n$ (see eq 3), we get

$$N_{\text{theo}} \approx 0.36 \frac{k}{\dot{\gamma}_c^n} \quad (23)$$

where the numerical coefficient was calculated in ref 13.

For the less concentrated solutions ($c = 10^{-5}$ g/g and $c = 10^{-4}$ g/g), the shear-thinning effect is too small to measure $\dot{\gamma}_c$. For the other solutions, the values for N deduced from the fit and from eq 23 are compared in Table 3 and found indeed to be comparable.

4. Concluding Remarks

When a fiber is coated out of a solution of polymer in the semidilute regime, the film is found to be swelled (by a factor of between 2 and 8), which is interpreted by considering the normal stress induced by the presence of the polymer. The (small) shear-thinning effect which could be induced by the polymer is found to be screened by this (large) effect. The solution of concentration 10^{-4} g/g (on the order of c^*) is of particular interest because it does not present any shear-thinning effect ($n \approx 1$) and has a viscosity close to the solvent one ($\eta = k \approx 1.2$ mPa·s). Nevertheless, a strong swelling effect is observed for this solution since the film is found to be 5 times thicker than if were made out of pure water.

The most concentrated solutions do not exhibit a sharp (inertial) increase of the thickness, since the withdrawal velocities remain smaller than 10 cm/s as it can be observed in Figure 3 (thus, inertia is always negligible). It should be of interest but remains to be done to study the coating with polymeric solutions at high velocity (where both inertial and non-Newtonian effects should combine), a case of practical importance in lubrication processes of glass and polymeric fibers.

Acknowledgment. It is a pleasure to thank Jean-Marc di Meglio and Sylvie Cohen-Addad for valuable discussions.

(13) Vinogradov, G. V.; Malkin, A. Ya. *Rheology of polymers*; Mir Publishers: Moscow, 1980.